Available online at www.sciencedirect.com

SciVerse ScienceDirect

Ceramics International 38 (2012) 2119–2123

CERAMICS INTERNATIONAL

www.elsevier.com/locate/ceramint

Correlation between crystal grain sizes of transparent ceramics and scintillation light yields

Akihiro Fukabori [a,*], Liqiong An [a], Akihiko Ito [a], Valery Chani [a], Kei Kamada [b], Akira Yoshikawa [a,c], Takayasu Ikegami [d], Takashi Goto [a]

[a] IMR, Tohoku University, 2-1-1, Katahira, Aoba-ku, Sendai, Miyagi 980-8577, Japan
[b] Furukawa Co., Ltd., 1-25-13, Kannondai, Tsukuba, Ibaraki 305-0856, Japan
[c] NICHe, Tohoku University, 6-6-10, Aoba-ku, Aramaki, Aoba-ku, Sendai, Miyagi 980-8579, Japan
[d] National Institute for Materials Science, 1-2-1, Sengen, Tsukuba, Ibaraki 305-0047, Japan

Received 7 September 2011; received in revised form 17 October 2011; accepted 18 October 2011
Available online 25 October 2011

Abstract

Light yields of Y_2O_3 ceramics are different from specimen to specimen. Nature of this phenomenon is not clear yet. Furthermore, origin of emission peaks for Y_2O_3 is not well understood. The results reported suggest that the emission derived from trapped excitons originates from the defects accumulated in the grain boundaries of the ceramics. In this paper, average grain size is introduced in order to evaluate defects inside the ceramics. Relationship between average crystal grain size and scintillation light yield is demonstrated.

Keywords: D. Y_2O_3; Scintillators; Transparent ceramics; Crystal grain size; Scintillation light yields

1. Introduction

Scintillators play important roles in various fields including nuclear medicine (positron emission tomography, X-ray computed tomography, and single photon emission computed tomography), high energy physics, geophysical and resource exploration, nuclear energy, and security fields (customs and homeland security). The scintillators emit light in visible and infrared regions of electromagnetic spectra by means of converting ionizing radiation (for example, α-ray, β-ray, γ-ray, X-ray, and neutrons) into a number of photons. This physical property is used to visualize interior characteristics of the objects and substances.

The scintillating properties required for the γ-ray scintillators are mostly high density, high effective atomic number, high transparency, high light yield (LY), and fast decay. The high light yield is often considered as most important condition of successful application of the scintillating material. Most of the existing commercial scintillators are single crystals grown from the melt by Czochralski and/or Bridgman methods. However, recently ceramic scintillators became also popular due to their excellent performance [1–4] considering their possible application as detectors of ionizing radiation.

In this project, Y_2O_3 ceramics were selected as a research object. This material has cubic structure, and therefore it does not demonstrate optical anisotropy. This is a reason why formation of highly transparent ceramics is possible. Furthermore, photo-absorption peaks were clearly detected in Y_2O_3 ceramics [2]. According to our observations, LYs of Y_2O_3 ceramics vary from specimen to specimen. This motivated us to examine correlation between structural properties of the ceramics and LY values.

The origin of the emission in undoped Y_2O_3 around 350 nm was reported to be self trapped excitons (STE) [2,5–12]. However, exact source of this emission peak is not finally determined yet, and it might be possible that the origin of these emission peaks is trapped excitons (TE). TE are trapped by defects including point defects, dislocations, grain boundaries (in the case of ceramics), and stacking faults. There is a chance that Y_2O_3 scintillation emission peaks around 350 nm are derived from the grain boundaries. In this case, there must be some relationship between LY and density of grain boundaries. For example, LY may increase with increasing or decreasing the number of grain boundaries. The aim of this communication was to discuss such relationship.

* Corresponding author.
E-mail address: akihirofukabori@gmail.com (A. Fukabori).

0272-8842/$36.00
doi:10.1016/j.ceramint.2011.10.052

2. Experimental methods

Polycrystalline Y_2O_3 transparent ceramics were produced by two methods. One was vacuum sintering via synthesizing fine precursor powder that is conventional method. Initially, the $Y(NO_3)_3$ starting solution was maintained at 1ow temperature. Then, drops of NH_{3aq} were added to the $Y(NO_3)_3$ solution. The drip rate for NH_{3aq} was optimized to obtain ready-to-sinter precursor powder. Thereafter, drops of $(NH_4)_3SO_4$ solution were added to avoid agglomeration of the powder. Finally, suction filtration was performed, and the precipitation was dispersed in distilled water to remove impurities. The resulting powder was calcined at 1080 °C or 1100 °C for 4 h in O_2 atmosphere to transform precursor into Y_2O_3. As a result of such treatment, fine and non-aggregated Y_2O_3 sinter-ability powder was produced. Green pellets were made from the powder under a pressure of 10 MPa using a tungsten carbide mold (as a preliminary step), and then pressed hydrostatically at 200 MPa. Thereafter, the pellets were isothermally sintered at 1700 °C and 1800 °C for 2 h at high vacuum in the furnace that was equipped with tungsten mesh heating elements. Finally, the pellets were lapped and polished. Details of the fabrication procedure were well described in the past [13].

Another technique used in this work was spark plasma sintering (SPS). Recently, this method has attracted much attention because it is considerably fast and allows grain boundary control and temperature gradient sintering. It also has low running cost. In the case of SPS ceramics, commercial Y_2O_3 (99.999%, High Purity Chemicals, Japan) powder was used as a starting material. This type ceramics were sintered using commercially available SPS apparatus (SPS-210LX, SPS Syntex, Japan) at 1300–1650 °C under 100 MPa pressure for 20–45 min using two step sintering [14,15]. The as-sintered SPS ceramics were colored black or grey due to presence of oxygen vacancies. Therefore, post-sintering heat treatments were necessary to fill up the structure (anion vacancies) with oxygen. This was performed at 980–1040 °C for 12 h in air.

Scanning electron microscope (SEM, Hitachi S-3400) and field emission scanning electron microscope (FE-SEM, JEOL JSM-7500F and Hitachi SU8000) were used to observe microstructure of the ceramics. In these characterizations, the back scattering electron (BSE) mode and secondary electron (SE) mode were used to inspect the surface of the ceramics and to visualize their grain structure and grain boundaries. The thermal electrons accelerated by voltage of about 10–20 kV and 2–15 kV were bombarded on the specimens, and the BSE (in the case of SEM) reflected on the surface and SE (in the case of FE-SEM) ejected from the sample were detected in low vacuum of 20–50 Pa and in high vacuum of 10^{-8} Pa, respectively. In the case of FE-SEM measurements, gold and platinum coating to the samples was carried out before observations. The degree of densification for the ceramics was examined through density measurements that were performed by the Archimedes method with distilled water. Average grain sizes were estimated using the Mendelson method with proportional constant of 1.56 [16].

Transmittance was examined at wavelengths range of 200–800 nm with UV–vis spectrophotometer (JASCO V550). Radio-luminescence (RL) spectra were recorded using FLS920 spectrofluorometer (Edinburgh Instruments) with corresponding spectral correction. The signals were accumulated by attaching the specimens on the surface of the radioactive ^{241}Am source (energy = 5.5 MeV, radioactivity = 4 MBq). To estimate LY under γ-ray excitation, the pulse height spectra were measured with a bias photo-multiplier tube (PMT, Hamamatsu Photonics R7600) under accelerating voltage of 700 V. The 662 keV γ-ray radiation from ^{137}Cs was used as excitation source. The samples were optically connected to the PMT window using optical grease (OKEN6262A). Output signal was transmitted to a pre-amplifier (ORTEC model 113), a shaping amplifier (ORTEC 572A) with 0.5 μs shaping time, a multi-channel analyzer (Amptek pocket MCA), and finally to a personal computer for the data analysis.

3. Results and discussion

Fig. 1 illustrates appearance of the Y_2O_3 ceramic pellets as produced by vacuum sintering (a and b) and by SPS technique at 1300 °C and 1650 °C during 45 min (c and d), respectively. It was assumed that scintillation properties cannot be evaluated accurately if considerable fraction of the pellets volume is empty due to presence of the pores. Therefore, degree of densification of all the ceramics shown in Fig. 1 was inspected by the Archimedes method. The relative densities were measured to be approximately 98.80% (for Y_2O_3-(a)), 99.4% (for Y_2O_3-(b)), 99.37% (for Y_2O_3-(c)), and 99.05% (for Y_2O_3-(d)). Thus, the densities of all the specimens were about 99%. This confirmed that both sintering processes introduced above resulted sufficient and practically complete densification of the materials discussed here.

Fig. 2 demonstrates SEM images of the surfaces of the ceramics. Grain and grain boundaries can be distinguished in all the images. The images (a) and (b) were observed by the SEM, and those indicated with (c) and (d) were obtained by the FE-SEM.

As it was mentioned in the introduction, there is a chance that grain boundaries accumulate considerable amount of the defects that support scintillating emission in the polycrystalline ceramics. Therefore, qualitative estimation of the density the grain boundary was necessary. However, direct evaluation of the density of the grain boundaries is difficult under present circumstances. Therefore, it was considered that average grain size could be adequate structural parameter representing the density of the grain boundaries. It is evident that both these parameters are closely related. Therefore, the average grain sizes were measured by Mendelson method for every sample using images similar to those seen in Fig. 2. The average grain sizes of these specimens were calculated to be about 17.55 μm (for Y_2O_3-(a)), 43 μm (for Y_2O_3-(b)), 0.43 μm (for Y_2O_3-(c)), and 1.9 μm (for Y_2O_3-(d)), respectively. Similarly, average crystal grain sizes of all other specimens produced in this study were estimated.

According to optical transmittance measurements, all the samples demonstrated high transparency around 60–80% at 700 nm as it is illustrated in Fig. 3. Radio-luminescence spectra

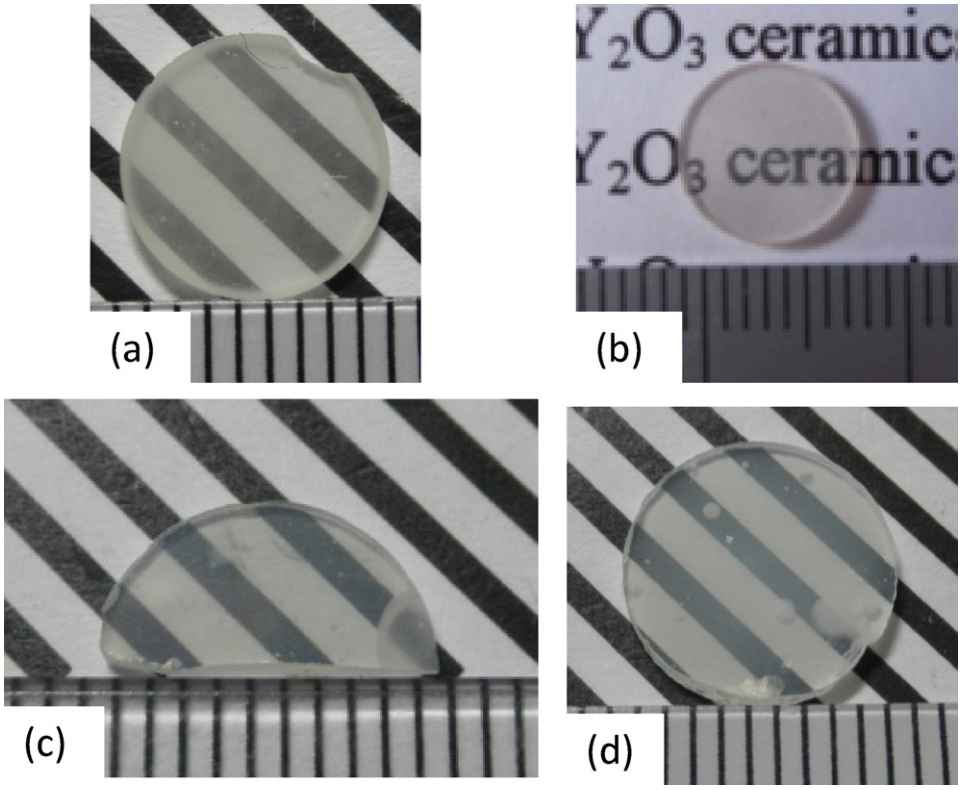

Fig. 1. View of the sintered compacts produced by vacuum sintering (Y_2O_3-(a) and Y_2O_3-(b)) and those produced by spark plasma sintering (Y_2O_3-(c) and Y_2O_3-(d)). Thicknesses of all ceramic specimens are 1 mm. Scale is in mm.

under ^{241}Am α-ray excitation were also recorded, and the center emission wavelengths were approximately 350 nm for all the samples (Fig. 4). This result correlates well with previous reports [2,5–12].

Fig. 5 presents the pulse height spectra recorded under ^{137}Cs 662 keV excitation. After photo-absorption peaks were fitted by the single Gaussian function in the pulse height spectra, the peak channels were determined. The LY for the specimen

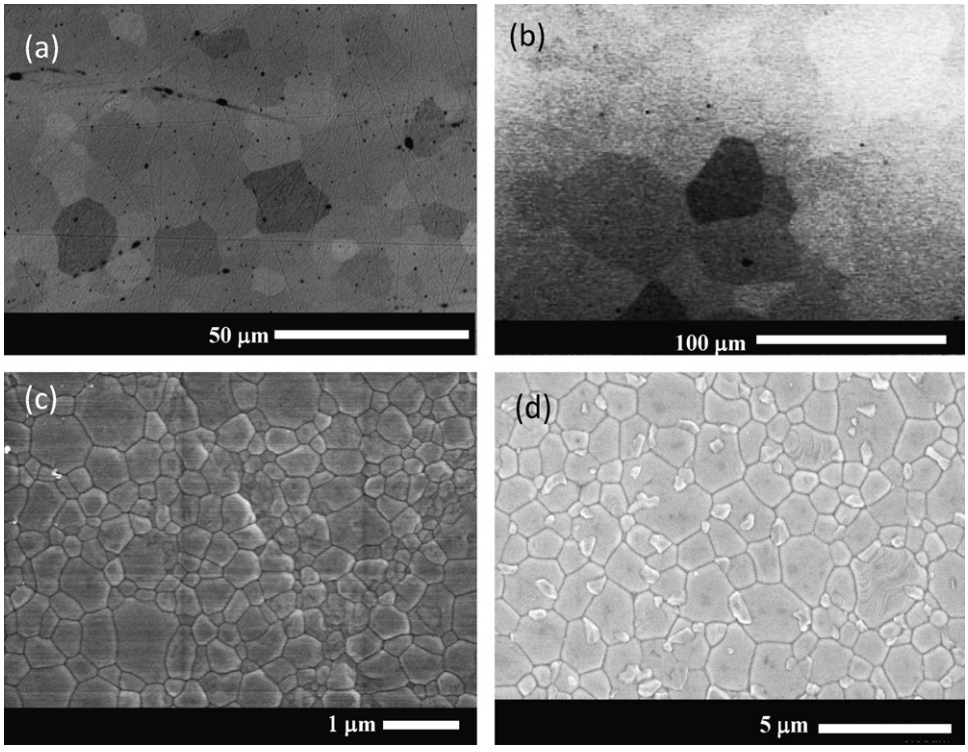

Fig. 2. SEM images of Y_2O_3 ceramics (See Fig. 1 for reference).

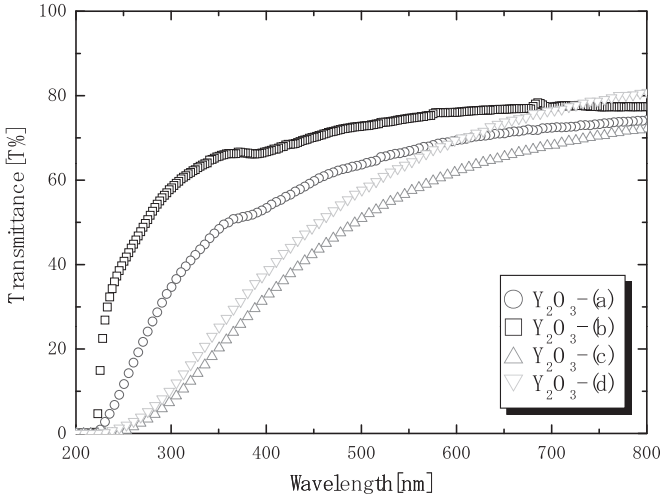

Fig. 3. Optical transmittance spectra from 200 nm to 800 nm (See Fig. 1 for reference).

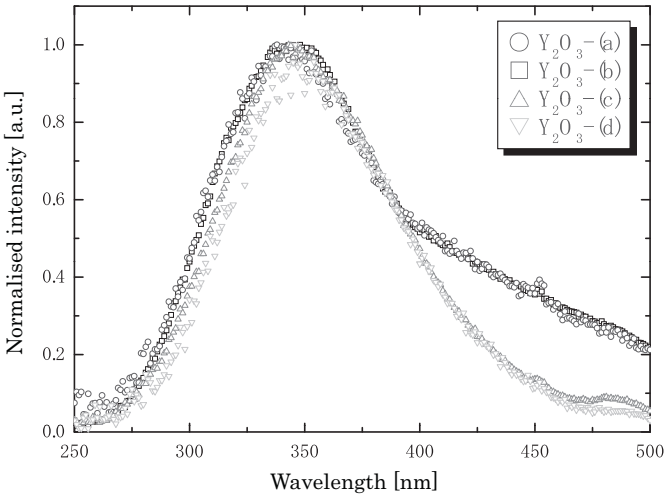

Fig. 4. Radio-luminescence spectra under ^{241}Am α-ray excitation after spectral correction (See Fig. 1 for reference).

Y_2O_3-(a) was 7400 ± 740 ph/MeV at room temperature. This value was calculated considering quantum efficiency (QE) of PMT and comparing channel at photo absorption peak of Y_2O_3-(a) with that of $Bi_4Ge_3O_{12}$ (BGO, LY: 8200 ph/MeV) [17] together with 10% error. The details of the calculation procedure are illustrated as follows:

$$\mathrm{LY} = 8200\ \text{photons/MeV} \times \frac{0.662\ \text{MeV}}{0.662\ \text{MeV}} \times \frac{0.32\ (\text{QE at}480\ \text{nm})}{0.45\ (\text{QE at}350\ \text{nm})} \times \frac{433}{342}(\text{channel}) = 7400 \times 740\ \text{photons/MeV}.$$

Similarly, LY values of other ceramics were calculated to be 9300 ± 930 ph/MeV (for Y_2O_3-(b)), 5100 ± 510 ph/MeV (for Y_2O_3-(c)), and 2300 ± 230 ph/MeV (for Y_2O_3-(d)). The LYs of all other specimens produced were also estimated. When the peak channels of the specimens were compared, it was found that peak center of Y_2O_3-(a) is larger than that of Y_2O_3-(b). Therefore, LY of Y_2O_3-(a) should be large, but the result was opposite. Pulse height spectra of Y_2O_3-(a) and Y_2O_3-(b) were measured at different days. Generally, peak channel of a same sample slightly changes depending on the measurement day. Therefore, peak center of Y_2O_3-(a) was larger. In order to evaluate exact LYs, BGO reference spectra were measured after every measurement.

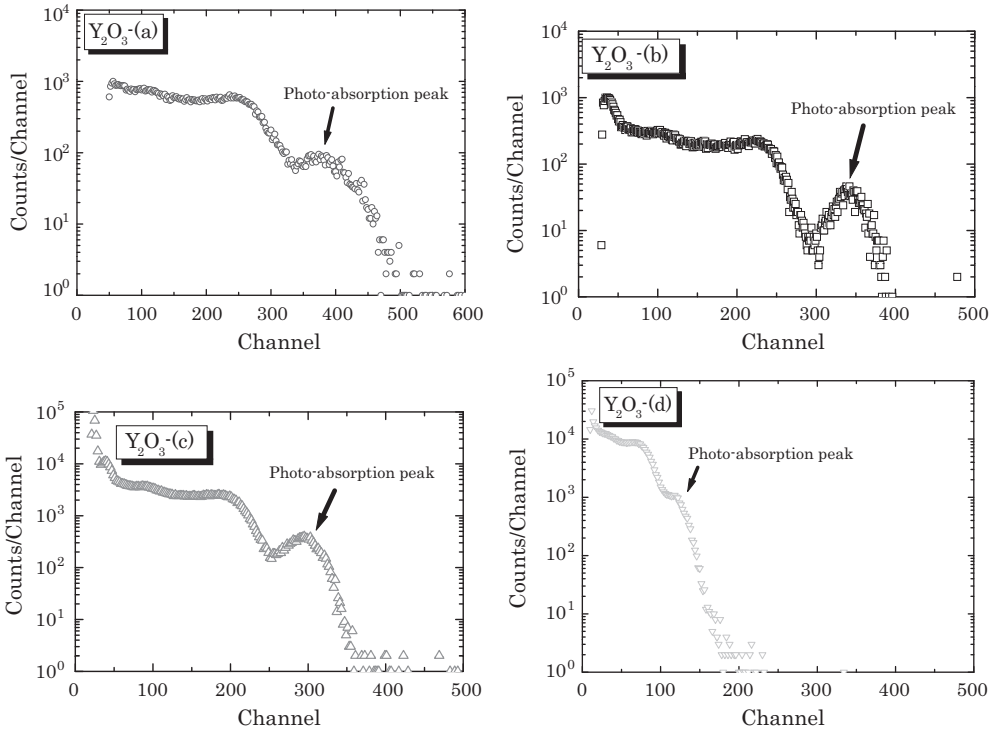

Fig. 5. Pulse height spectra under ^{137}Cs γ-ray excitation (See Fig. 1 for reference).

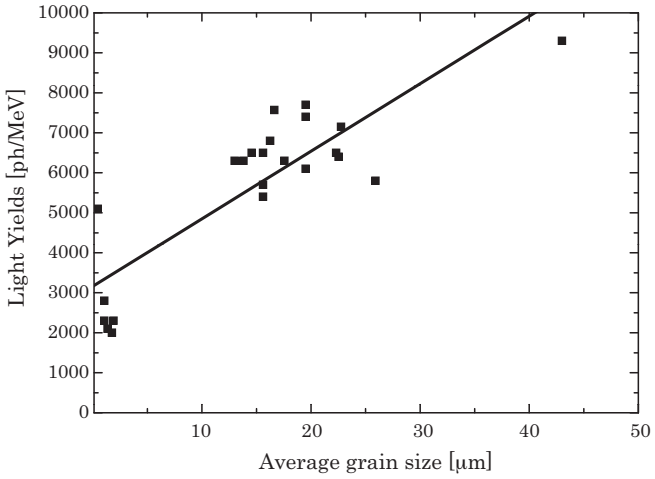

Fig. 6. Correlation between scintillation light yields of the Y_2O_3 ceramic specimens and their average grain sizes. Solid line is fitting line.

The optical transmittance of the SPS ceramics at emission wavelength of approximately 350 nm was lower than that of the vacuum sintered samples. Therefore, there is a chance that lower LY was observed in the SPS ceramics as a result of re-absorption effect compared with vacuum sintered samples. However, in this study, the LYs were not corrected for contribution of transmittance. The density of Y_2O_3 is 5.04 g/cm^3 that is not sufficiently high. As a result, γ-ray can penetrate deep inside to the vicinity of exit surface. Thus, scintillation light was also emitted in the region of exit face. In the measurements reported here, the optical transmittance was evaluated by simply comparing intensity of the incident light with that of the output light. Considering these circumstances, correction by multiplied LY by optical transmittance value is not always accurate. Therefore, this correction was not performed. It is assumed that derivation of more precise correlation between LY and crystal grain size is possible when the specimens produced by both methods with similar transmittance above 70% are available.

Correlation between LY and the average grain size is illustrated in Fig. 6. As it was mentioned above, the average grain size represents number of the defects accumulated on the grain boundaries. According to Fig. 6, LY increases with increasing average grain size. It indicates that the number of the defects supporting the emission is intimately related to the number of the grain boundaries. Currently, it is not possible to make final decision about relationship between the density of the grain boundaries and the emission because ascription of emission is not finally concluded yet.

Furthermore, considering rare earth doped ceramics, it is not evident that similar correlation can be concluded. This issue should be studied additionally [18]. Moreover, the ceramics discussed above were produced by two different methods. This is additional factor that may have effect on performance of the materials as scintillators. Nevertheless, this report was mostly focused on the relationship between average grain size and the light yield.

4. Conclusions

It was found that light yield increases with increasing average grain size of the transparent Y_2O_3 ceramics. Thus, it was concluded that the defects supporting the emission are related to the grain boundaries.

Acknowledgments

This project was supported by Global Center of Excellence program for ‘‘Materials Integration’’, Tohoku University, Japan. One of the authors (A.F.) appreciate the useful advice of M. Kitaura of Yamagata University.

References

[1] C. Greskovich, S. Duclos, Ceramic scintillators, Annu. Rev. Mater. Sci. 27 (1997) 69.
[2] A. Fukabori, T. Yanagida, J. Pejchal, S. Maeo, Y. Yokota, A. Yoshikawa, T. Ikegami, F. Moretti, K. Kamada, Optical and scintillation characteristics of Y_2O_3 transparent ceramics, J. Appl. Phys. 107 (2010) 073501.
[3] E. Zych, C. Brecher, A.J. Wojtowicz, H. Lingertat, Luminescence properties of Ce-activated YAG optical ceramic scintillator materials, J. Lumin. 75 (1997) 193.
[4] E. Zych, C. Brecher, H. Lingertat, Host-associated luminescence from YAG optical ceramics under gamma and optical excitation, J. Lumin. 78 (1998) 121.
[5] N. Ogorodnikov, A.V. Kruzhalov, V.Y. Ivanov, Mechanism of fast UV-scintillations in oxide crystals with self-trapped excitons, Proceedings of International Conference on Inorganic Scintillator and their Applications, SCINT95.
[6] W. Hayes, Mechanism of exciton trapping in oxides, J. Lumin. 31–32 (1984) 99.
[7] A.I. Kuznetsov, V.N. Abramov, N.S. Rooze, T.I. Savikhina, Autolocalized excitons in Y_2O_3, JETP Lett. 28 (1978) 602.
[8] W. Hayes, M.J. Kane, O. Salminen, A.I. Kuznetsov, An ODMR study of exciton trapping in Y_2O_3 and Sc_2O_3, J. Phys. C: Solid State Phys. 17 (1984) L383.
[9] G. Blasse, L.H. Brixner, The nature of the luminescence of Y_2O_3 and Sc_2O_3, Eur. J. Solid State Inorg. Chem. 28 (1991) 767.
[10] A. Lushchik, M. Kirm, Ch. Lushchik, I. Martinson, G. Zimmerer, Luminescence of free and self-trapped excitons in wide-gap oxides, J. Lumin. 87–89 (2000) 232.
[11] R.L. Wood, W. Hayes, A study of recombination centers in $YAlO_3$ $EuAlO_3$, $LaAlO_3$ and Y_2O_3 using ODMR, J. Phys. C: Solid State Phys. 15 (1982) 7209.
[12] N.V. Guerassimova, I.A. Kamenskikh, D.N. Krasikov, V.V. Mikhailin, K. Petermann, D.F. de Sousa, G. Zimmerer, Charge transfer luminescence of Yb^{3+} and intrinsic luminescence in sesquioxides Lu_2O_3, Y_2O_3, Sc_2O_3 and Yb_2O_3, HASYLAB Annual Reports, 2005.
[13] A. Fukabori, M. Sekita, T. Ikegami, N. Iyi, T. Komatsu, M. Kawamura, M. Suzuki, Induced emission cross section of a possible laser line in Nd:Y_2O_3 ceramics at 1.095 μm, J. Appl. Phys. 101 (2007) 043112.
[14] L. An, A. Ito, T. Goto, Fabrication of transparent lutetium oxides by spark plasma sintering, J. Am. Ceram. Soc. 94 (2011) 695.
[15] L. An, A. Ito, T. Goto, Two-step pressure sintering of transparent lutetium oxide by spark plasma sintering, J. Eur. Ceram. Soc. 31 (2011) 1597.
[16] M.I. Mendelson, Average grain size in polycrystalline ceramics, J. Am. Ceram. Soc. 52 (1969) 443.
[17] M. Moszynski, T. Ludziejewski, D. Wolski, W. Klamra, L.O. Norlin, Properties of YAG:Ce scintillator, Nucl. Instrum. Methods A 345 (1994) 461.
[18] R. Feigelson, Challenge in preparing high optical quality ceramics for laser and scintillator application, Invited Oral Presentation, The 18th American Conference on Crystal Growth and Epitaxy (ACCGE), 31 July–5 August 2011, Monterey, CA.